Heliyon 5 (2019) e02152

Contents lists available at ScienceDirect

Heliyon

journal homepage: www.heliyon.com

Preparation and evaluation of ZnO nanoparticles by thermal decomposition of MOF-5

Shirin Hajiashrafi [a], Negar Motakef Kazemi [b,*]

[a] Department of Pharmaceutical Chemistry, Faculty of Pharmaceutical Chemistry, Tehran Medical Sciences, Islamic Azad University, Tehran, Iran
[b] Department of Medical Nanotechnology, Faculty of Advanced Sciences and Technology, Tehran Medical Sciences, Islamic Azad University, Tehran, Iran

ARTICLE INFO

Keywords:
Inorganic chemistry
Materials chemistry
Nanotechnology

ABSTRACT

In recent years, the use of zinc oxide nanoparticles (ZnO NPs) has attracted considerable attention due to its unique properties. In this study, ZnO nanoparticles were synthesized by a simple and repeatable method with thermal decomposition of a zinc-based metal organic framework (Zn-MOF). MOF-5 was prepared by solution (at room temperature) and solvothermal (at 90 °C) methods in dimethylformamide (DMF) as a solvent via the self-assembly of zinc acetate and dehydrate benzene-1,4-dicarboxylate (BDC) as metal ion center and organic bridging ligand respectively without and with tri-ethylamine (TEA) as capping agent. The result products were characterized by Fourier transform infrared (FTIR) for investigation functional groups, X-ray diffraction (XRD) for determination of crystalline structure, scanning electron microscope (SEM) for evaluation of size and morphology, energy-dispersive X-ray spectroscopy (EDS) for determination of chemical composition, and diffuse reflection spectroscopy (DRS) for investigation of Ultraviolet (UV) protective properties. The antibacterial activities of ZnO NPs were studied against *Escherichia coli* (*E. coli*).

1. Introduction

Nanotechnology has received broad attention because of its distinctive properties and applications. Nanostructured has become one of the most important of material with unique properties duo to small size and high surface area [1]. ZnO has been one of the hottest topics in recent years due to their unique properties and potential applications [2, 3, 4, 5, 6]. Nanostructured zinc oxide materials have become one of attractive research fields due to expansion of application in different aspects [7]. Zinc oxide nanomaterials are one of richest nanostructures in terms of variety of morphology and application [8, 9]. Based on condition and synthesis method, ZnO nanostructures were observed with different shapes such as nanoneedles [10], nanowires [11, 12, 13, 14, 15], nanorods [16], nanotubes [17, 18], nanobelts [19], nanosheets [20, 21, 22], nanoparticles [23, 24, 25, 26], and nanowhiskers [27]. Much efforts have been devoted to different methods of zinc oxide nanostructures synthesis with tunable size and shape such as sol–gel [28], green synthesis [29], hydrothermal [30, 31], laser ablation [32], pyrolysis [33], ionic liquid precursor [34], sonochemical [35], and thermal decomposition [36, 37].

Nanostructures play an important role to improve the electronic properties including sensing, production efficiency, catalysis, etc. These materials have been widely investigated as key to achieve the ultra-high response [38, 39]. Photodetector is one of the important applications of nanomaterials with high-performance to develop large-area UV broadband [40, 41]. Zinc oxide nanomaterial has attracted much consideration for their potential applications in many areas [42, 43]. The use of zinc oxide has expanded for design and manufacture of UV photodetectors [44, 45]. Recently, UV blocking application has extended for ZnO nanoparticles. The regions of UV radiation are included UV-A (320–400 nm), UV-B (280–320 nm), and UV-C (180–280 nm) that protection of them can be important role on safety [8, 46]. Other application of ZnO NPs has been the major role of them in significant interest worldwide for antibacterial activity with focus on their safety and effectiveness against Gram-positive and Gram-negative bacteria [8, 47]. Zinc oxide nanoparticles were often acted through destruction mechanism of bacterial wall similar to other nanoparticles as the most important antibiotics [48].

Thermal decomposition of Zn-MOF is one of new route of methods for ZnO NPs synthesis [49]. Metal organic framework, also known as porous coordination polymer, has attracted much special scientific attention due to their unique properties and emerging applications in recent years. MOF is composed of a three-dimensional (3D) network of organic-inorganic crystalline hybrid [50, 51]. Metal organic frameworks are synthesized via self-assembly method from the coordination of polydendate ligands as organic sectors and metal ions (or metal clusters) as

* Corresponding author.
E-mail address: motakef@iaups.ac.ir (N. Motakef Kazemi).

https://doi.org/10.1016/j.heliyon.2019.e02152
Received 30 March 2019; Received in revised form 16 June 2019; Accepted 22 July 2019

inorganic sectors. MOFs have been attracted wide interest duo to large surface area, high pore volume, and adjustable shape and pore [52]. Zinc-based metal organic framework is expanding as one of the most popular metal–organic coordination polymers. The controlled size and shape of Zn-MOF can be developed according to ligand type and the preparation conditions for various applications [53, 54]. MOF-5 was reported by Omar M. Yaghi in 1999 as Zn-MOF that synthesized by connection of Zn_4O units and 1,4-benzenedicarboxylate ligands to form a cubic network with the formula $Zn_4O(BDC)_3$ [55]. Zinc-based metal organic framework can be synthesized by solution and solvothermal methods [56, 57]. Recently, the effect of temperature and capping agent was reported on the size of MOF-5 [58]. In this work, zinc oxide nanoparticles were prepared by thermal decomposition of prepared MOF-5 without and with tri-ethylamine by solution and solvothermal methods. The objective of the present study was to develop the effect of prepared ZnO NPs on UV blocking and antibacterial activity applications.

2. Materials and methods

2.1. Materials

All chemicals used were analytical grade. Ultra-pure water was used for the preparation of all reagents solutions. The materials used for the synthesis of the ZnO NPs were purchased: zinc acetate dehydrate ($Zn(O_2CCH_3)_2(H_2O)_2$) as the zinc precursor, terephthalic acid ($C_6H_4(CO_2H)_2$) as ligand, tri-ethylamine ($N(CH_2CH_3)_3$) as capping agent, dimethylformamide (C_3H_7NO) as solvent from Merck (Germany).

2.2. Synthesis of ZnO nanoparticles

The MOFs were prepared without and with capping agent via solution and solvothermal method for 2.5 h based on previous report [35]. The samples called MOF-5 (I), MOF-5 (II), MOF-5 (III), and MOF-5 (IV) in condition without TEA at room temperature, with TEA at room temperature, without TEA at 90 °C, and with TEA at 90 °C respectively. Then, ZnO nanoparticles were synthesized by thermal decomposition of MOFs in an air atmosphere at 550 °C for 5 hours. Thermal decomposition of MOFs as porous materials was caused to remove the organic ligand and the form the primary nuclei of zinc oxide nanoparticles. At the result, ZnO nanoparticles were not porous, and the size can be related to the synthesis conditions of MOF-5 included temperature and presence and absence of the capping agent.

2.3. Characterization

The samples were characterized by Fourier transform infrared, X-ray powder diffraction, dynamic light scattering, scanning electron microscope, X-ray diffraction, UV blocking, and antibacterial activity. Fourier transform infrared spectrum was recorded on a Unicam Matson 1000 FT-IR spectrophotometer using a KBr disks at room temperature. The X-ray diffraction was used for determination of crystalline structure of nanoparticles utilizing Cu Kα X-ray radiation with a voltage of 40 kV and a current of 30 mA by X'pert pro diffractometer (ASENWARE, AW-XBN300, China). Scanning electron microscope was applied for investigation of size and morphology of nanoparticles (KYKY, EM3200, China). Energy-dispersive X-ray spectroscopy was evaluated the elemental and chemical analysis (ASK SEM-CL View VIS, Oxford instruments, UK). Diffuse reflection spectroscopy was evaluated the UV protective of nanoparticles (UV2550, Shimadzu). The antibacterial activities were studied by disk diffusion method against *Escherichia coli* as Gram-negative bacteria (ATCC 1399, Islamic Azad University).

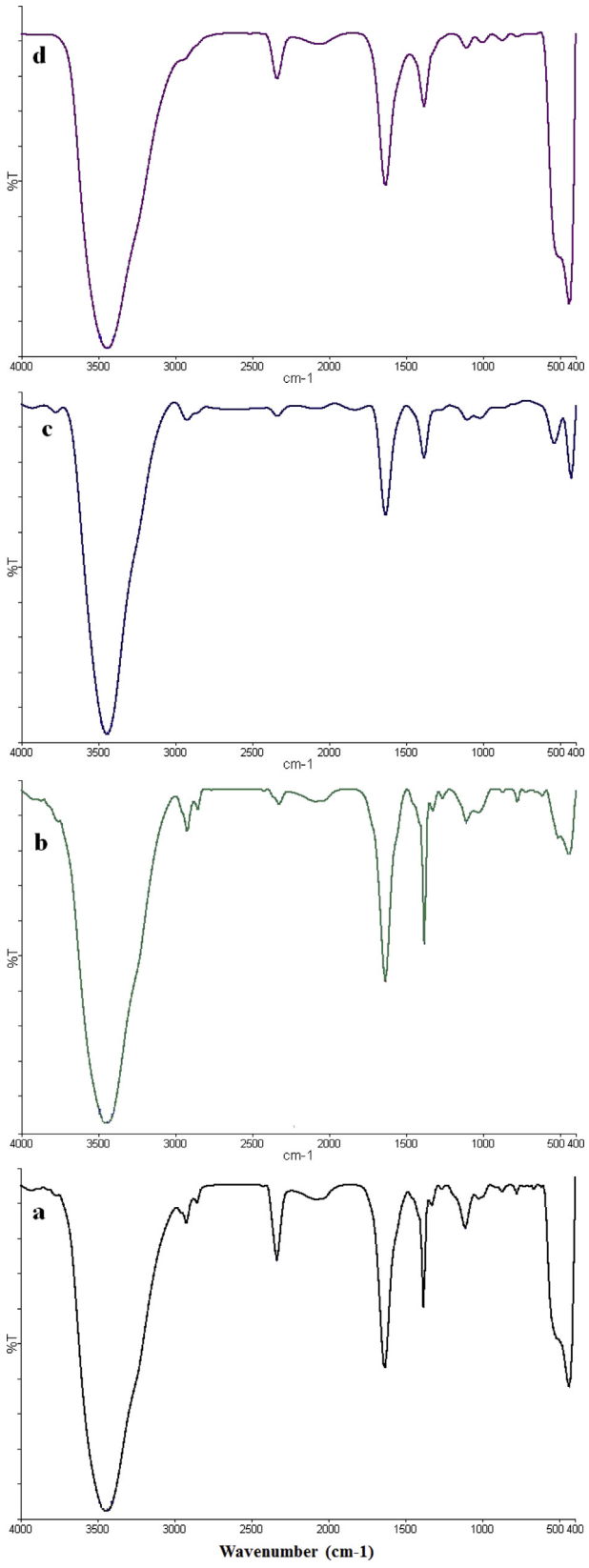

Fig. 1. FTIR spectra of prepared ZnO NPs from a) MOF-5 (I), b) MOF-5 (III), c) MOF-5 (II), and d) MOF-5 (IV).

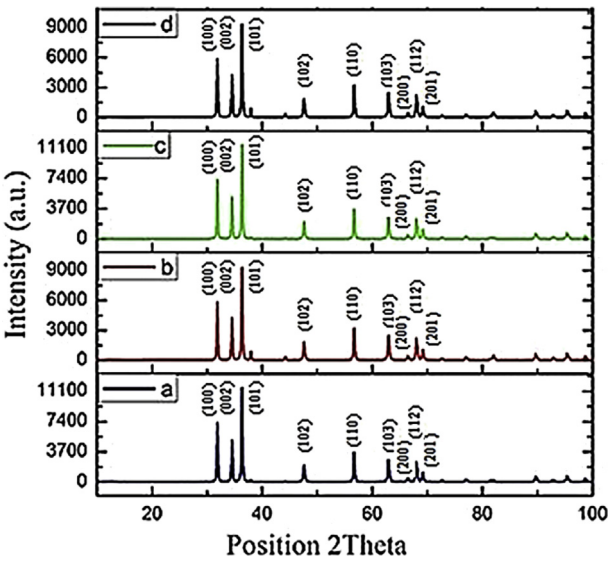

Fig. 2. XRD Pattern of prepared ZnO NPs from a) MOF-5 (I), b) MOF-5 (III), c) MOF-5 (II), and d) MOF-5 (IV).

3. Results and discussions

3.1. FTIR

The IR absorption spectra of metal–organic frameworks were presented in previous report [54]. The FTIR absorption spectrum of zinc nanoparticle was recorded in the range of 400–4000 cm^{-1} (Fig. 1). The O–H stretching vibrations appeared at 3440 cm^{-1}. The peak at 2341 cm^{-1} is related to CO_2 which exist in environment. The peak at 1385–1630 cm^{-1} is related to nitrate (NO_3^-) group. The absorption band at 431–444 cm^{-1} is confirmed the formation of ZnO NPs from metal-oxygen (Zn–O) vibration. Fourier transform infrared result is similar to a previously reported pattern [47]. Based on the results, the peaks of resulting from the presence of ligands in MOFs were deleted which it is a qualitative confirmation of the synthesis of ZnO nanoparticles.

3.2. XRD

X-ray diffraction of MOFs were presented in previous report which conformed to the standard card [54]. X-ray diffraction of zinc nanoparticles was measured from to 10–100° (2θ), which approved the crystalline structure (Fig. 2). The characteristic peaks were observed at 31.78, 34.44, 36.28, 47.55, 56.62, 62.83, 66.21°, 67.96°, and 68.10° (2θ angle) corresponding to crystal planes (100), (002), (101), (102), (110), (103), (200), (112), and (201) respectively. Based on the XRD results, ZnO NPs were correctly synthesized and crystalline structure was similar to the previously reported pattern (JCPDS card No. 36–1451) [8]. Based on the XRD results, characteristic peaks of nanoparticles were corresponding with the crystalline structure ZnO, and was not observed characteristic peaks of MOFs as a precursor.

3.3. SEM

The SEM images of prepared ZnO nanoparticles are shown in Fig. 3. The ligands were destroyed by thermal decomposition method of MOFs at 550 °C for 5 hours and formed the primary nuclei of zinc oxide nanoparticles based on the synthesis conditions. SEM results were shown ZnO nanoparticles with spherical shape in nanometer scale. ZnO NPs show the average size of 110 nm for MOF-5 (I), 90 nm for MOF-5 (II), 100 nm for MOF-5 (III), and 80 nm for MOF-5 (VI). Based on SEM results, the smaller size of particles was observed in presence capping agent and temperature. In synthesis of MOFs, TEA as capping agent has prevented the growth of particles by blocking the crystalline plates, and resulted to the formation of MOFs with smaller size. Higher temperature for synthesis of MOFs was caused more nucleation of metal ion center, and the increasing of self-assembly for the formation of MOFs. As a result, thermal decomposition of smaller MOF was caused the formation of smaller ZnO nanoparticles.

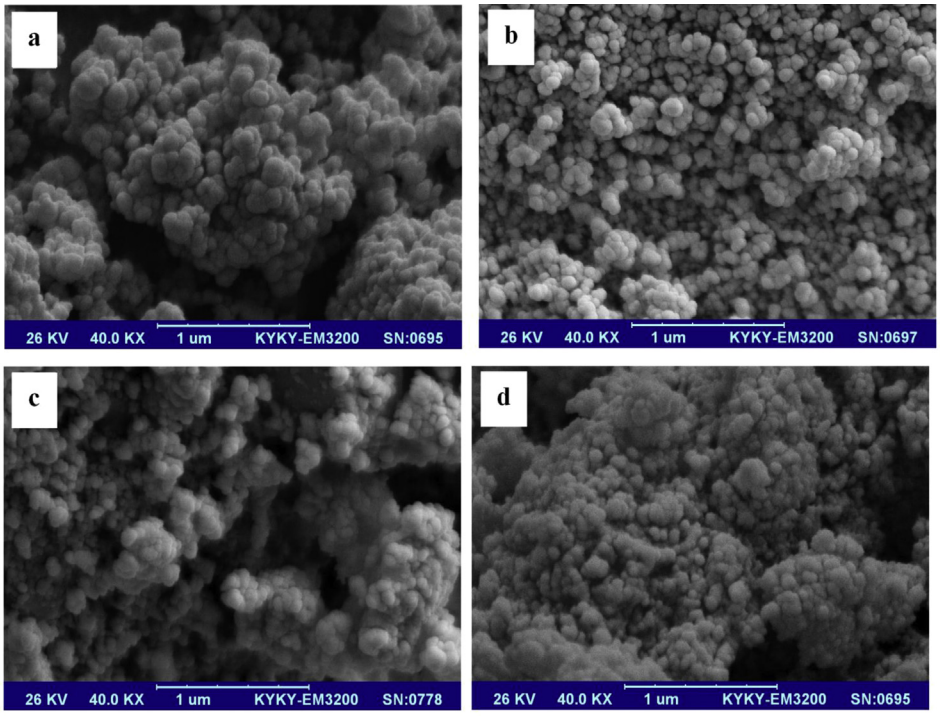

Fig. 3. SEM images of prepared ZnO NPs from a) MOF-5 (I), b) MOF-5 (III), c) MOF-5 (II), and d) MOF-5 (IV).

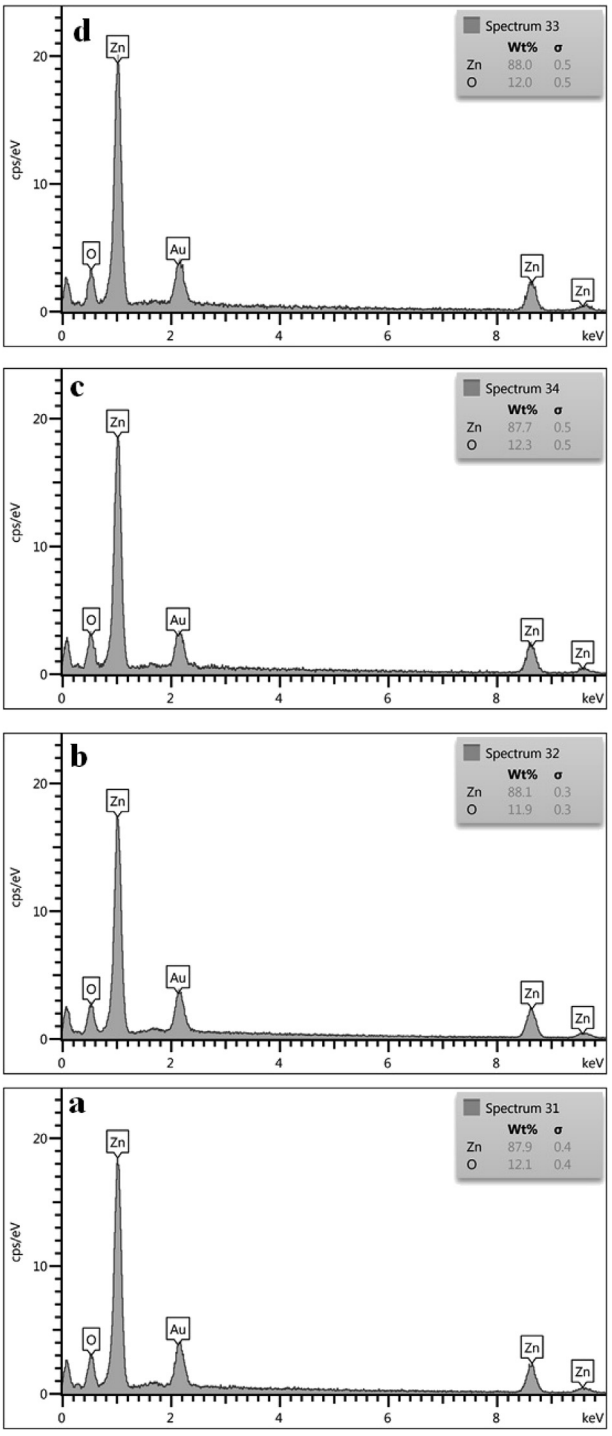

Fig. 4. EDS of prepared ZnO NPs from a) MOF-5 (I), b) MOF-5 (III), c) MOF-5 (II), and d) MOF-5 (IV).

3.4. EDS

The X-ray diffraction spectroscopy was used to evaluate the chemical composition of zinc oxide nanoparticle. This analysis was clearly showed the identification strong peaks of zinc (Zn) and oxygen (O) elements and no other impurities are present. The EDS analysis of zinc oxide NP exhibited absorption bands with peaks at 1.0, 8.6, and 9.6 keV, which illustrated a typical absorption of the metallic zinc. Composition analysis of pure ZnO nanoparticles was reported in Fig. 4. The X-ray diffraction spectroscopy results were corresponding with previous reports [58, 59].

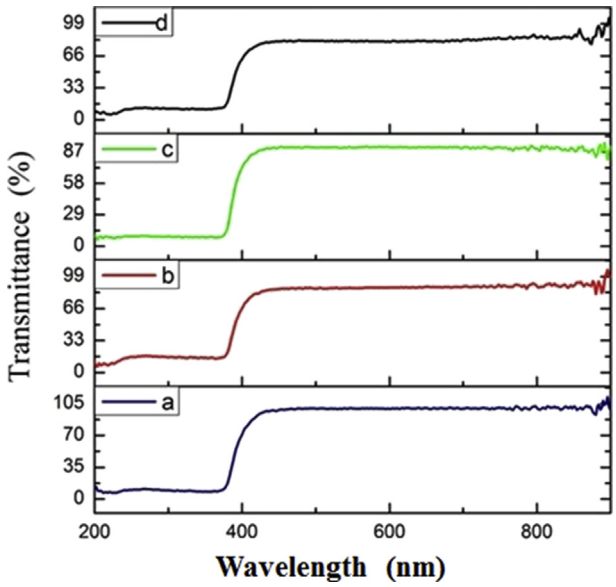

Fig. 5. DRS absorption rate of prepared ZnO NPs from a) MOF-5 (I), b) MOF-5 (III), c) MOF-5 (II), and d) MOF-5 (IV).

Table 1
Antibacterial activity of ZnO NPs.

MOF-5 (IV)	MOF-5 (III)	MOF-5 (II)	MOF-5 (I)	ZnO NPs from MOF-5
8.6	3.5	8.1	3.14	The zone inhibition (mm)

3.5. DRS

Diffuse reflection spectroscopy was used to characterize the optical properties [58, 59]. The absorption spectra of nanoparticles were recorded in the wavelength range of 200–800 nm in diffuse reflectance mode. The DRS absorption spectra of ZnO NPs showed the absorption peak observed in range of 200–400 nm. Based on the results, UV protective properties of ZnO nanoparticles approved in three Ultraviolet: UV-A, UV-B, and UV-C (Fig. 5). The diffuse reflection spectroscopy results were corresponding with previous reports [8].

3.6. Antibacterial activity

Antibacterial activity of prepared ZnO NPs was investigated against *Escherichia Coli* as Gram-negative bacteria by agar diffusion method with constant concentration (0.01 g/ml). Based on the zone inhibition, the more antibacterial activity was observed for ZnO NPs with smaller size in presence of capping agent and higher temperature (Table 1). The effect of temperature was corresponding with previous reports for antibacterial activity results [8]. According to previous report, the antibacterial activity is influenced by particle size, concentration, morphology, surface modifications. The main mechanisms of antibacterial activity for ZnO NPs are including: the direct contact with cell walls and the destruction of bacterial cell, the generation of reactive oxygen species (ROS), and release of antimicrobial ions mainly Zn^{2+} ions [60]. In this study, the effective factors on antibacterial activity can be release NO^{3-} (caused by TEA) and Zn^{2+} (caused by a zinc cluster) ions, and metallic Zn. Based on the results, the TEA effect for MOF synthesis was more specified than temperature effect on antibacterial activity.

4. Conclusion

The zinc oxide nanoparticles synthesized by thermal decomposition of prepared MOF-5 in different conditions. The XRD spectrum confirmed

the pure ZnO crystalline structure for all samples. SEM results showed homogeneous nanoparticles with spherical morphology. In the present study, we successfully observed UV blocking and antibacterial activity applications of ZnO NPs. Thermal decomposition method of MOF can be used as a simple approach for the preparation of nanoparticles to different application fields such as food, pharmaceutical, cosmetic, agriculture and textile industries and become a major area of research for other nanoparticle preparation in the future.

Declarations

Author contribution statement

Shirin Hajiashrafi: Performed the experiments; Analyzed and interpreted the data; Contributed reagents, materials, analysis tools or data; Wrote the paper.

Negar Motakef Kazemi: Conceived and designed the experiments; Analyzed and interpreted the data; Contributed reagents, materials, analysis tools or data; Wrote the paper.

Funding statement

This research did not receive any specific grant from funding agencies in the public, commercial, or not-for-profit sectors.

Competing interest statement

The authors declare no conflict of interest.

Additional information

No additional information is available for this paper.

References

[1] G.A. Ozin, Nanochemistry: synthesis in diminishing dimensions, Adv. Mater. 4 (10) (1992) 612–649.
[2] V.I. Korepanov, S. Yuan Chan, H.C. Hsu, H. Hamaguchi, Phonon confinement and size effect in Raman spectra of ZnO nanoparticles, Heliyon 5 (2) (2019), e01222.
[3] R. Bhardwaj, A. Bharti, J.P. Singh, K. Hwa, N. Goyal, S. Gautam, Structural and electronic investigation of ZnO nanostructures synthesized under different environments, Heliyon 4 (4) (2018), e00594.
[4] K. Hu, F. Teng, L. Zheng, P. Yu, Z. Zhang, H. Chen, X. Fang, Binary response Se/ZnO p-n heterojunction UV photodetector with high on/off ratio and fast speed, Laser Photonics Rev. 11 (1) (2017) 1600257.
[5] B. Zhao, F. Wang, H. Chen, L. Zheng, L. Su, D. Zhao, X. Fang, An ultrahigh responsivity (9.7 mA W−1) self-powered solar-blind photodetector based on individual ZnO–Ga_2O_3 heterostructures, Adv. Funct. Mater. 27 (17) (2017) 1700264.
[6] F. Teng, L. Zheng, K. Hu, H. Chen, Y. Li, Z. Zhang, X. Fang, Surface oxide thin layer of copper nanowires enhanced the UV selective response of a ZnO film photodetector, J. Mater. Chem. C 36 (4) (2016) 8416–8421.
[7] Z.L. Wang, Zinc oxide nanostructures: growth, properties and applications, J. Phys. Condens. Matter 16 (2004) R829–R858.
[8] A. Kołodziejczak-Radzimska, T. Jesionowski, Zinc oxide—from synthesis to application: a review, Materials 7 (2014) 2833–2881.
[9] S. Hajiashrafi, N. Motakef-Kazemi, Green synthesis of zinc oxide nanoparticles using parsley extract, Nanomed. Res. J. 3 (1) (2018) 44–50.
[10] J.L. Yang, S.J. An, W.I. Park, G.C. Yi, W. Choi, Photocatalysis using ZnO thin films and nanoneedles grown by metal–organic chemical vapor deposition, Adv. Mater. 16 (18) (2004) 1661–1664.
[11] C.J. Lee, T.J. Lee, S.C. Lyu, Y. Zhang, H. Ruh, H.J. Lee, Field emission from well-aligned zinc oxide nanowires grown at low temperature, Appl. Phys. Lett. 81 (19) (2002) 3648–3650.
[12] X. Wang, Q. Li, Z. Liu, J. Zhang, Z. Liu, R. Wang, Low-temperature growth and properties of ZnO nanowires, Appl. Phys. Lett. 84 (24) (2004) 4941–4943.
[13] H.T. Ng, J. Han, T. Yamada, P. Nguyen, Y.P. Chen, M. Meyyappan, Single crystal nanowire vertical surround-gate field-effect transistor, Nano Lett. 4 (2004) 1247–1252.
[14] M.H. Huang, S. Mao, H. Feick, H. Yan, Y. Wu, H. Kind, E. Weber, R. Russo, P. Yang, Room-temperature ultraviolet nanowire nanolasers, Science 292 (5523) (2001) 1897–1899.
[15] M. Law, L.E. Greene, J.C. Johnson, R. Saykally, P. Yang, Nanowire dye-sensitized solar cells, Nat. Mater. 4 (6) (2005) 455.
[16] J.J. Wu, S.C. Liu, Catalyst-free growth and characterization of ZnO nanorods, J. Phys. Chem. B 106 (37) (2002) 9546–9551.
[17] J.Q. Hu, Q. Li, X.M. Meng, C.S. Lee, S.T. Lee, Thermal reduction route to the fabrication of coaxial Zn/ZnO nanocables and ZnO nanotubes, Chem. Mater. 15 (1) (2003) 305–308.
[18] X. Wang, Y. Ding, C.J. Summers, Z.L. Wang, Large-scale synthesis of six-nanometer-wide ZnO nanobelts, J. Phys. Chem. B 108 (26) (2004) 8773–8777.
[19] Z.W. Pan, Z.R. Dai, Z.L. Wang, Nanobelts of semiconducting oxides, Science 291 (2001) 1947–1949.
[20] X.W. Sun, L.D. Wang, H.S. Kwok, Improved ITO thin films with a thin ZnO buffer layer by sputtering, Thin Solid Films 360 (1-2) (2000) 75–81.
[21] J. Lv, W. Gong, K. Huang, J. Zhu, F. Meng, X. Song, Z. Sun, Effect of annealing temperature on photocatalytic activity of ZnO thin films prepared by sol–gel method, Superlattice Microstruct. 50 (2) (2011) 98–106.
[22] B.L. Zhu, X.Z. Zhao, F.H. Su, G.H. Li, X.G. Wu, J. Wu, R. Wu, Low temperature annealing effects on the structure and optical properties of ZnO films grown by pulsed laser deposition, Vacuum 84 (11) (2010) 1280–1286.
[23] S.D. Lee, S.H. Nam, M.H. Kim, J.H. Boo, Synthesis and photocatalytic property of ZnO nanoparticles prepared by spray-pyrolysis method, Phys. Procedia 32 (2012) 320–326.
[24] P. Banerjee, S. Chakrabarti, S. Maitra, B.K. Dutta, Zinc oxide nano-particles–sonochemical synthesis, characterization and application for photo-remediation of heavy metal, Ultrason. Sonochem. 19 (1) (2012) 85–93.
[25] C.H. Hsieh, Spherical zinc oxide nano particles from zinc acetate in the precipitation method, J. Chin. Chem. Soc. 54 (1) (2007) 31–34.
[26] K. Foe, G. Namkoong, T.M. Abdel-Fattah, H. Baumgart, M.S. Jeong, D.S. Lee, Controlled synthesis of ZnO spheres using structure directing agents, Thin Solid Films 534 (2013) 76–82.
[27] J.Q. Hu, Y. Bando, Growth and optical properties of single-crystal tubular ZnO whiskers, Appl. Phys. Lett. 82 (2003) 1401–1403.
[28] X. Ma, A. Liu, H. Xu, G. Li, M. Hu, G. Wu, Preparation of large-scale highly oriented ZnO noodle arrays and study on the photoconductivity, Curr. Nanosci. 4 (2008) 157–160.
[29] N. Bala, S. Saha, M. Chakraborty, M. Maiti, S. Das, R. Basub, P. Nandy, Green synthesis of zinc oxide nanoparticles using *Hibiscus subdariffa* leaf extract: effect of temperature on synthesis, anti-bacterial activity and anti-diabetic activity, RSC Adv. 5 (2015) 4993–5003.
[30] K.S. Kim, H. Jeong, M.S. Jeong, G.Y. Jung, Polymer-templated hydrothermal growth of vertically aligned single-crystal ZnO nanorods and morphological transformations using structural polarity, Adv. Funct. Mater. 20 (2010) 3055–3063.
[31] B.J. Li, L.J. Huang, M. Zhou, N.F. Ren, Morphology and wettability of ZnO nanostructures prepared by hydrothermal method on various buffer layers, Appl. Surf. Sci. 286 (2013) 391–396.
[32] G. Al-Dahash, W. Mubdir Khilkala, Preparation and characterization of ZnO nanoparticles by laser ablation in NaOH aqueous solution, Iran. J. Chem. Chem. Eng. (Int. Engl. Ed.) 37 (1) (2018) 11–16.
[33] F. Xu, M. Dai, Y. Lu, L. Sun, Hierarchical ZnO nanowire−nanosheet architectures for high power conversion efficiency in dye-sensitized solar cells, J. Phys. Chem. C 114 (2010) 2776–2782.
[34] C. Ge, Z. Bai, M. Hu, D. Zeng, S. Cai, C. Xie, Synthesis and gas-sensing properties of ZnO particles from an ionic liquid precursor, Mater. Lett. 62 (2008) 2307–2310.
[35] A. Esmaielzadeh Kandjani, M. Farzalipour Tabriz, B. Pourabbas, Sonochemical synthesis of ZnO nanoparticles: the effect of temperature and sonication power, Mater. Res. Bull. 43 (2008) 645–654.
[36] C.C. Lin, Y.Y. Li, Synthesis of ZnO nanowires by thermal decomposition of zinc acetate dehydrate, Mater. Chem. Phys. 113 (1) (2009) 334–337.
[37] F.Z. Karizi, V. Safarifard, S.K. Khani, A. Morsali, Ultrasound-assisted synthesis of nano-structured 3D zinc (II) metal–organic polymer: precursor for the fabrication of ZnO nano-structure, Ultrason. Sonochem. 23 (2015) 238–245.
[38] W. Kong, Q. Miao, Y. Lei, Multimodal sensor medical image fusion based on local difference in non-subsampled domain, IEEE Trans. Electron Devices 66 (2019) 938–951.
[39] A. Alarawi, V. Ramalingam, H.C. Fu, P. Varadhan, R. Yang, J.H. He, Enhanced photoelectrochemical hydrogen production efficiency of MoS_2-Si heterojunction, Opt. Express 27 (8) (2019) A352–A363.
[40] W. Yang, K. Hu, F. Teng, J. Weng, Y. Zhang, X. Fang, High-performance silicon-compatible large-area UV-to-Visible broadband photodetector based on integrated lattice-matched type II Se/n-Si heterojunctions, Nano Lett. 18 (8) (2018) 4697–4703.
[41] Y. Zhang, W. Xu, X. Xu, J. Cai, W. Yang, X. Fang, Self-powered dual-color UV–green photodetectors based on SnO_2 millimeter wire and microwires/$CsPbBr_3$ particle heterojunctions, J. Phys. Chem. Lett. 10 (4) (2019) 836–841.
[42] S. Anandan, A. Vinu, T. Mori, N. Gokulakrishnan, P. Srinivasu, V. Murugesan, K. Ariga, Photocatalytic degradation of 2, 4, 6-trichlorophenol using lanthanum doped ZnO in aqueous suspension, Catal. Commun. 8 (9) (2007) 1377–1382.
[43] M. Sabbaghan, A.A. Firooz, V.J. Ahmadi, The effect of template on morphology, optical and photocatalytic properties of ZnO nanostructures, J. Mol. Liq. 175 (2012) 135–140.
[44] Z. Zhang, Y. Ning, X. Fang, From nanofibers to ordered ZnO/NiO heterojunction arrays for self-powered and transparent UV photodetector, J. Mater. Chem. C7 (2) (2019) 223–229.

[45] Y. Ning, Z. Zhang, F. Teng, X. Fang, Novel transparent and self-Powered UV photodetector based on crossed ZnO nanofiber Array homojunction, Small 14 (2018) 1703754.
[46] T.G. Smijs, S. Pavel, Titanium dioxide and zinc oxide nanoparticles in sunscreens: focus on their safety and effectiveness, Nanotechnol. Sci. Appl. 4 (2011) 95–112.
[47] A. Sirelkhatim, S. Mahmud, A. Seeni, N.H.M. Kaus, L. Chuo Ann, S. Khadijah Mohd Bakhori, H. Hasan, D. Mohamad, Review on zinc oxide nanoparticles: antibacterial activity and toxicity mechanism, Nano-Micro Lett. 7 (3) (2015) 219–242.
[48] F. Hossain, O.J. Perales-Perez, S. Hwang, F. Roman, Antimicrobial nanomaterials as water disinfectant: applications, limitations and future perspectives, Sci. Total Environ. 466–467 (2014) 1047–1059.
[49] F.S. Shirazi, K. Akhbari, Preparation of zinc oxide nanoparticles from nanoporous metal–organic framework with one-dimensional channels occupied with guest water molecules, Inorg. Chim. Acta 436 (2015) 1–6.
[50] A.U. Czaja, N. Trukhan, U. Muller, Industrial applications of metal–organic frameworks, Chem. Soc. Rev. 38 (2009) 1284–1293.
[51] J.L.C. Rowsell, O.M. Yaghi, Metal–organic frameworks: a new class of porous materials, Microporous Mesoporous Mater. 73 (2004) 3–14.
[52] J.D. Sosa, T.F. Bennett, K.J. Nelms, B.M. Liu, R.C. Tovar, Y. Liu, Metal–organic framework hybrid materials and their applications, Crystals 8 (2018) 325–348.
[53] N. Motakef-Kazemi, S.A. Shojaosadati, A. Morsali, *In situ* synthesis of a drug-loaded MOF at room temperature, Microporous Mesoporous Mater. 186 (2014) 73–79.
[54] M.R. Mehmandoust, N. Motakef-Kazemi, F. Ashouri, Nitrate adsorption from aqueous solution by metal–organic framework MOF-5, Iran. J. Sci. Technol. Trans. A-Science 43 (2) (2018) 443–449, 2019.
[55] H. Li, M. Eddaoudi, M. O'Keeffe, O. Yaghi, Design and synthesis of an exceptionally stable and highly porous metal-organic framework, Nature 402 (1999) 276–279.
[56] N. Motakef-Kazemi, S.A. Shojaosadati, A. Morsali, Evaluation of the effect of nanoporous nanorods $Zn_2(bdc)_2(dabco)$ dimension on ibuprofen loading and release, J. Iran. Chem. Soc. 13 (7) (2016) 1205–1212.
[57] D.J. Tranchemontagne, J.R. Hunt, O. Yaghi, Room temperature synthesis of metal-organic frameworks: MOF-5, MOF-74, MOF-177, MOF-199, and IRMOF-0, Tetrahedron 64 (2008) 8553–8557.
[58] H. Sarma, D. Chakrabortty, K.C. Sarma, Structural and optical properties of ZnO nano particles, IOSR J. Appl. Phys. 6 (4) (2014) 8–12.
[59] S.S. Kumar, P. Venkateswarlu, V.R. Rao, G.N. Rao, Synthesis, characterization and optical properties of zinc oxide nanoparticles, Int. Nano Lett. 3 (30) (2013) 1–6.
[60] A. Sirelkhatim, S. Mahmud, A. Seeni, N.H.M. Kaus, L.C. Ann, S.K.M. Bakhori, H. Hasan, D. Mohamad, Review on zinc oxide nanoparticles: antibacterial activity and toxicity mechanism, Nano-Micro Lett. 7 (3) (2015) 219–242.